European Journal of Pharmaceutics and Biopharmaceutics 155 (2020) 22–28

Contents lists available at ScienceDirect

European Journal of Pharmaceutics and Biopharmaceutics

journal homepage: www.elsevier.com/locate/ejpb

Functionalised calcium carbonate as a coformer to stabilize amorphous drugs by mechanochemical activation

Jingwen Liu[a], Thomas Rades[a], Ingunn Tho[b], Eric Ofosu Kissi[b,*]

[a] Department of Pharmacy, Faculty of Health and Medical Science, University of Copenhagen, Universitetsparken 2, DK-2100 Copenhagen, Denmark
[b] Department of Pharmacy, The Faculty of Mathematics and Natural Sciences, University of Oslo, P.O. Box 1068, Blindern 0371, Oslo, Norway

ARTICLE INFO

Keywords:
Physical stability
Amorphous
Amorphization
Porous
Functionalized calcium carbonate
Drug release

ABSTRACT

The aim of this study was to investigate the amorphization, physical stability and drug release of a model drug, carvedilol (CAR), when loaded onto functionalised calcium carbonate (FCC) using mechanochemical activation (vibrational ball milling). The solid-state characteristics and physical stability of CAR–FCC samples, prepared at different weight ratios and for different milling times, were determined using differential scanning calorimetry and X-ray powder diffraction. Upon milling CAR–FCC samples containing 50% CAR, amorphization of CAR was observed after 10 min. For CAR–FCC samples milled for either 30 or 90 min, it was found that CAR was amorphised at all ratios (10–90% CAR), but FCC remained crystalline. The glass transition temperature ($T_{g\alpha}$) of the various CAR–FCC samples milled for 90 min was found to be similar (38 °C) for all ratios containing 20% CAR and above. The similar $T_{g\alpha}$s for the different drug ratios indicate deposition of amorphous CAR onto the surface of FCC. For CAR–FCC samples containing 10% CAR, a $T_{g\alpha}$ of 49 °C was found, which is 11 °C higher compared with other CAR–FCC samples. This may indicate restricted molecular mobility resulting from CAR molecules that are in close contact with the FCC surface. The physical stability, under both stress (100 °C) and non-stress conditions (25 °C at dry conditions), showed that drug concentrations up to 30% CAR can be stabilized in the amorphous form for at least 19 weeks under non-stress conditions when deposited onto FCC, compared to less than a week physical stability of neat amorphous CAR. *In vitro* drug release showed that CAR–FCC samples containing 60% CAR and below can improve the drug release and generate supersaturated systems compared to neat amorphous and crystalline CAR. Samples with lower drug concentrations (40% CAR and below) can maintain supersaturation during 360 min of dissolution testing. This study indicates that the crystalline inorganic material, FCC, can facilitate amorphization of drugs, provide stabilization against drug crystallization, and improve dissolution properties of amorphous drugs upon mechanochemical activation.

1. Introduction

Solubility and permeability of a drug are crucial properties that determine the oral bioavailability of a drug, and form the basis of the biopharmaceutics drug classification system [1–3]. However, many crystalline drugs exhibit poor aqueous solubility due to their molecular crystalline order and the associated high energy required for molecules to overcome the crystalline lattice and go into solution [4–6]. In view of this, amorphous drug delivery systems have been developed as one strategy to overcome poor aqueous solubility, increase apparent solubility and improve bioavailability for these so-called “brick dust” molecules [7,8]. However, only a few commercially available dosage forms have been developed containing neat amorphous drug (*e.g.* Ceftin® (cefuroxime axetil), Accolate® (zafirlukast), Viracept® (nelfinavir mesylate), Crestor® (rosuvastatin Ca), Accupril® (quinapril HCl) [9]). This is because amorphous drugs, *i.e.* materials that lack long-range orientational and positional molecular order [9,10], exhibit mobility even at very low temperatures, below the glass transition temperature ($T_{g\alpha}$) but above the so-called β-relaxation temperature ($T_{g\beta}$) [11]. The presence of a low $T_{g\beta}$ means that most amorphous drugs will revert over time to their respective crystalline form making most neat amorphous drugs practically physically unstable [11].

Arguably, physical instability is the main reason that most drugs are not developed in the amorphous form in standard capsules and tablets [12]. However, there are several ways how amorphous drugs can be prevented from recrystallization. One approach is to form a glass solution, *i.e.* a single-phase amorphous system of the drug and another component [13]. Glass solutions can be classified according to whether

* Corresponding author.
E-mail address: e.o.kissi@farmasi.uio.no (E.O. Kissi).

https://doi.org/10.1016/j.ejpb.2020.07.029
Received 14 April 2020; Received in revised form 23 June 2020; Accepted 24 July 2020
Available online 05 August 2020

a polymer or a non-polymeric excipient is used as the second component (coformer) to stabilize the amorphous drug [14,15]. For a polymeric glass solution, the drug molecules can be dissolved (molecularly dispersed) in an amorphous polymer matrix to form an amorphous solid dispersion [16,17]. The stabilization provided by polymers is based on the thermodynamic solubility of the drug in the polymer [18], but also drug concentrations above the solubility limit of the drug compound in the polymer can be stable for some time [19].

Non-polymeric glass solutions involve the use of small molecules such as amino acids [20], organic acids [21], dipeptides [22], or a second drug [23–25], to stabilize the amorphous form of the drug. The resulting formulations are referred to as a co-amorphous [26]. Co-amorphous systems are thus formed by the amorphization of two or more low molecular weight, initially crystalline starting materials, and are characterised by a single $T_{g\alpha}$ [15]. Stabilization of amorphous drugs in co-amorphous systems is based on intimate mixing, hindrance of molecular mobility and interactions between the different molecules [15,27,28].

Another promising stabilization approach is the deposition of drug molecules into the pores or onto the surface of porous inorganic materials. These porous materials, including mesoporous silica [29,30], calcium carbonate [31], and calcium phosphate [31], provide a large surface area for drug molecules to be loaded onto for drug delivery purposes [30–33]. In previous work on amorphous stabilization using mesoporous silica, it could be shown that the deposited drug molecules form hydrogen bonds with the surface molecules of their host particles. This bonding, which is as strong as that found in crystalline drugs, together with spatial confinement of the drug molecules in pores of the mesoporous silica provide stabilization against drug crystallization [34].

A porous inorganic compound, which may exhibit the desired characteristics for amorphous physical stabilization and improvement of drug dissolution is functionalised calcium carbonate (FCC). FCC is a specifically engineered micro-particle pigment for rapid absorption and high liquid uptake [35]. FCC is highly porous and has micro- to nanopore sizes, and hence, provides a high surface area for drug loading [32]. In the field of pharmaceutics, FCC has been investigated for the delivery of proteins using a solvent loading method [36], as drug carrier using solvent evaporation [32] and to produce orally dispersible tablets [37].

Methods of loading drugs into or onto excipients or carriers can be classified into wet and dry loading methods. Wet loading involves dissolving the drug usually in an organic solvent or solvent mixture followed by quick evaporation of the solvent in the presence of excipient or carrier (solvent evaporation techniques) [38]. Wet loading is fast but a potential limitation is the presence of residual solvent. Methods that do not use solvents to get the drug amorphised are termed as dry loading methods, *e.g.,* sublimation of drug onto or into carriers [39], melting, and mechanochemical activation techniques such as milling [38]. Mechanochemical activation of amorphous drugs by milling is a green approach to amorphization and circumvents problems with residual solvent. Milling follows the so-called kinetic pathway of converting drugs into an amorphous form [10]. During milling, crystalline defects are gradually induced until the crystalline lattice is lost. This causes the drug molecules to arrange randomly and amorphization is achieved [10,40]. In the context of the current work, milling, might also expose nanopores present in the internal structure of FCC particles [32], and might create a larger surface area available for drug loading.

In this study, we explore the possibility of using mechanochemical activation (using a vibrational ball mill) to co-mill and investigate amorphization of the model drug carvedilol (CAR), its physical stabilization and its drug release using crystalline inorganic FCC as a coformer. We show that by mechanochemical activation with FCC, the drug amorphization time can be reduced significantly and the physical stability of amorphous CAR can be increased from less than a week to at least 19 weeks (experimental time of the stability study). Additionally, we show that FCC improves the drug release properties during dissolution and facilitates the formation and maintenance of a supersaturated drug concentration, compared to pure amorphous drug.

2. Materials and methods

2.1. Materials

FCC (Omyapharm® 500-OG) was obtained from Omya International AG (Oftringen, Switzerland) (average particle size = 6.6 μm), and CAR (polymorphic form II, Cambridge Structural Database Refcode: GIVJUQ01) was obtained from Fagron (Copenhagen, Denmark). Sodium dihydrogen phosphate dihydrate and di-sodium hydrogen phosphate heptahydrate were purchased from Merck (Darmstadt, Germany). All materials were used as received.

2.2. Methods

2.2.1. Samples preparation

A total mass of 1000 mg powder, containing the starting materials CAR or FCC, and physical mixtures (PM) of CAR and FCC at different drug to excipient weight ratios (10–90% CAR), were placed into 25 mL milling jars containing two stainless steel balls with a diameter of 12 mm. The samples were milled at a frequency of 30 Hz for either 30 or 90 min in an oscillatory ball mill (Mixer Mill MM400, Retsch GmbH & Co., Haan, Germany), kept in a cold room (5 °C). For samples milled for 90 min, milling was intermittently stopped after 10, 20, 30 and 60 min for sampling. The final CAR and FCC mixtures after milling were termed CAR–FCC and the different ratios are classified in terms of weight percent of the drug content, *e.g.,* 20% CAR. Samples prepared for this study can be generally grouped as; *i.* samples (CAR, FCC and CAR–FCC containing 50% CAR) milled for 90 min and analysed based on the milling time, *ii.* samples (CAR–FCC) milled for 90 min and characterised based on their percentage drug content and, *iii.* samples (CAR and CAR–FCC) milled for 30 min for physical stability and *in vitro* drug release analysis.

2.2.2. X-ray powder diffraction (XRPD)

XRPD measurements were performed using an X'Pert PANalytical PRO X-ray diffractometer (PANalytical, Almelo, The Netherlands). Cu Kα radiation (λ = 1.54187 Å) was generated using a 45 kV acceleration voltage and current of 40 mA. Samples were scanned in reflectance mode from 5–38° 2θ with a scan rate of 0.067° 2θ/s and a step size of 0.026° 2θ. The data was collected and analyzed using the software X'Pert Data Collector (version 2.2.4) (PANalytical, Almelo, The Netherlands).

2.2.3. Differential scanning calorimetry (DSC)

The thermal properties of the samples were investigated using a DSC822 (Mettler-Toledo, Switzerland) coupled with a refrigerated cooling accessory. Powder samples of approximately 2–6 mg were weighed into 4 μL aluminium crucibles and sealed with perforated lids. The measurements were conducted in standard temperature mode, with a heating rate of 10 °C/min. CAR–FCC samples were heated from 0 to 140 °C. Milled neat FCC samples were analysed using a Discovery DSC (TA Instruments, New Castle, USA) at a heating rate of 10 °C/min from 0 to 350 °C. $T_{g\alpha}$ values were determined from the midpoint of the characteristic sigmoidal step change in the heat flow signal.

2.2.4. Scanning electron microscopy

The morphology of the samples was determined using a Hitachi TM3030 Tabletop scanning electron microscope (SEM, Hitachi High-Technologies Corporation, Tokyo, Japan). The samples were mounted on an aluminium tab using a conductive carbon tape, and sputter-coated with a gold layer. The microscope parameters were set to an accelerating voltage of 15 kV and 1000 × magnification.

2.2.5. Physical stability test

CAR–FCC samples containing 10–80% CAR milled for 90 min were stored in a Memmert UF55 oven (Schwabach, Germany) for 2 h at 100 °C and the samples were then analysed immediately with XRPD.

CAR–FCC samples containing 10–90% CAR milled for 30 min were stored in a desiccator under dry conditions over silica gel at 25 °C. Samples were regularly analyzed by XRPD (weekly for the first 5 weeks, and every two weeks thereafter) until recrystallization of CAR was detected from the XRPD diffractograms.

2.2.6. Dissolution

Non-sink powder dissolution studies were performed in a scaled-down USP2 apparatus consisting of a set of mini glass vessels with rotating mini paddles (ERWEKA DT70, Heusenstamm, Germany) [41]. A volume of 100 mL of 0.1 M phosphate buffer (pH 7.2, 37 °C) was used as dissolution medium and the rotation speed of mini paddles was set to 100 rpm. For CAR–FCC samples containing 20, 30, 40, 50, 60 and 80% CAR (milled for 30 min), a powder sample containing a total of 100 mg of CAR was used for dissolution. 5 mL aliquots were collected at 1, 3, 5, 10, 15, 20, 40, 60, 90, 120, 180, 240 and 360 min of dissolution and immediately replaced with pre-warmed fresh dissolution medium, and quantified by UV spectroscopy at 330 nm after filtration (filter pore size: 0.45 μm). All experiments were conducted in triplicate.

3. Results and discussion

3.1. Amorphization of CAR in the presence of an equal weight ratio of FCC

Amorphous drugs are characterised by the absence of diffraction peaks and the presence of a broad signal typically called the “amorphous halo” in their XRPD diffractograms. To determine the amorphization of CAR in the presence of FCC, the pure starting materials (CAR and FCC) and an equal weight ratio of the starting materials (CAR–FCC sample containing 50% CAR) were milled for 90 min and the solid state of the samples was determined after different milling times by XRPD.

3.1.1. Solid state changes during milling of the starting materials

The diffractograms indicating solid state changes of the starting materials during milling are shown in Fig. 1. For pure CAR (Fig. 1a), significant reduction in peak intensities can be observed after 10 min of milling. After 20 min of milling, no peaks were visible in the diffractogram, indicating that CAR requires between 10 and 20 min of mechanochemical activation via vibrational ball milling to convert from the crystalline state to the amorphous form.

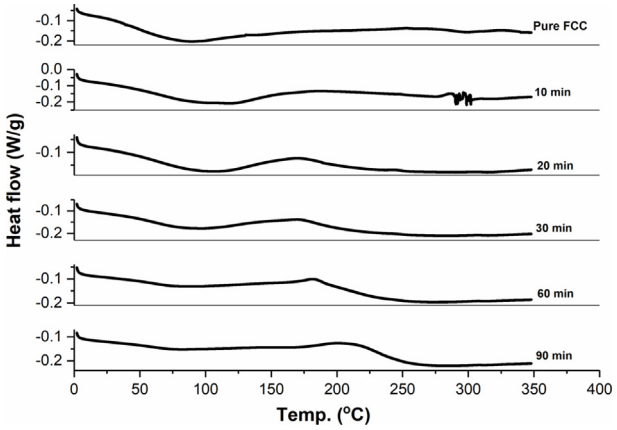

Fig. 2. Thermograms of FCC after different milling times showing the absence of a major transition signals.

For FCC, a decrease in XRPD peak intensity and disappearance of minor peaks with increasing milling time is shown in Fig. 1b. Peak height and area reduction can be observed at 25.9, 29.0 and 32.0 °2θ with peaks at 23.0 and 36.0 °2θ disappearing after 90 min of milling. Reduction in peak intensity and disappearance of peaks after milling are usually associated with increasing amorphous content [42]. However, due to the irregular reduction pattern and the presence of peaks after 90 min of milling, this is more likely to be due to particle size reduction (see SEM images in Fig. S1 in supporting information). In order not to rule out the presence of amorphous FCC, due to the absence of some diffraction peaks after 90 min of milling, a DSC analysis was performed on FCC samples during a total of 90 min of milling and the thermograms are shown in Fig. 2. The thermograms show broad transitions between 25 and 180 °C for all FCC samples, which can be attributed to the evaporation of moisture from the surface and pores of FCC particle. No clear $T_{g\alpha}$ signal can be determined from the thermograms that would suggest that FCC did become amorphous.

3.1.2. Solid state changes of CAR–FCC sample containing 50% CAR during 90 min milling

An equal weight ratio of CAR and FCC was milled together to

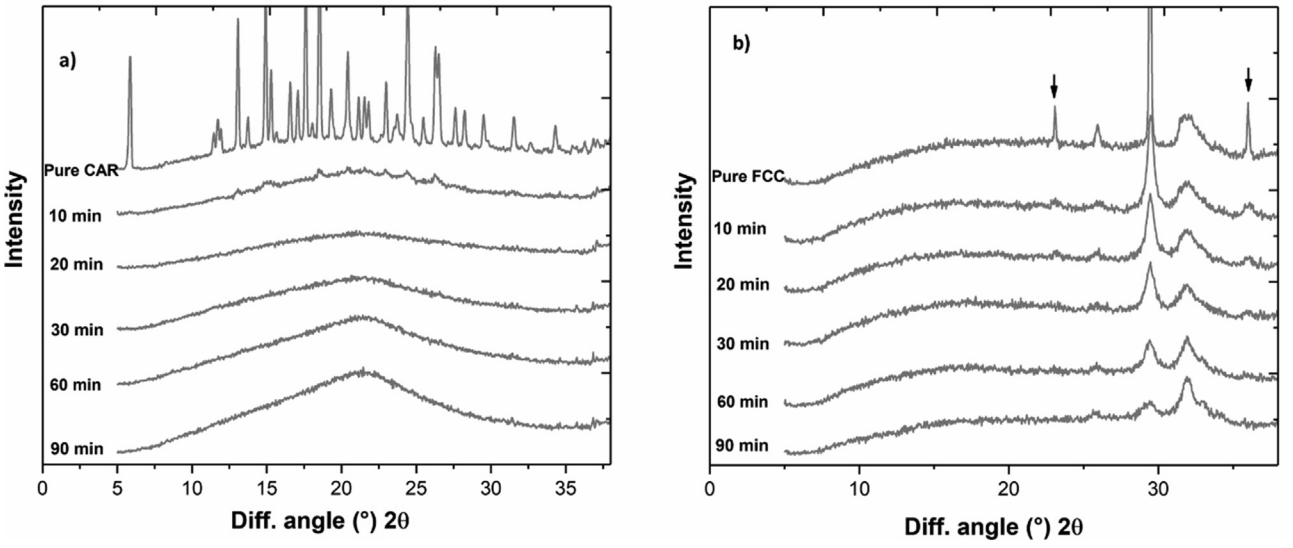

Fig. 1. Diffractorgrams of a) CAR and b) FCC showing peak reduction and amorphization after different milling times. Arrows indicate FCC peaks that disappear after 90 min of milling.

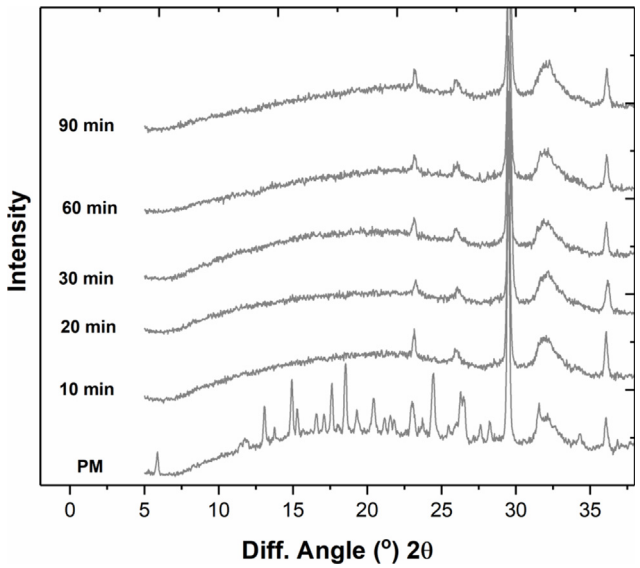

Fig. 3. Diffractograms of a CAR–FCC sample containing 50% CAR after milling for different times. In addition, the physical mixture of FCC and CAR showing crystalline peaks of the starting materials is shown.

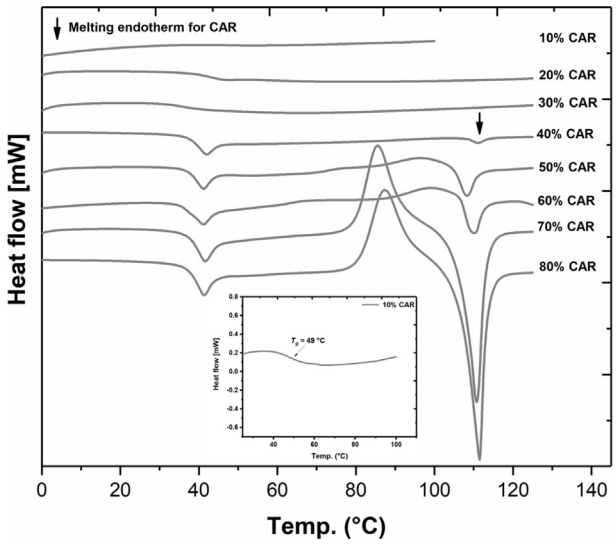

Fig. 4. DSC thermograms of various CAR–FCC samples showing similar $T_{g\alpha}$ signal and samples where a melting endotherm of CAR is observed. The inset shows a zoomed-in thermogram of the CAR–FCC sample containing 10% CAR.

determine amorphization of CAR in the presence of FCC. The XRPD diffractograms for the CAR–FCC samples at various time points are shown in Fig. 3. The PM of CAR and FCC showed their respective crystalline forms. The diffractogram of the sample after 10 min of milling reveals crystalline peaks of FCC but no peaks of crystalline CAR. The diffractograms after 20, 30, 60 and 90 min of milling also showed an absence of crystalline CAR related peaks, whilst peaks between 25 and 38° 2θ, belonging to FCC, were still present. The disappearance of CAR peaks can be attributed to the amorphization of the drug. This initial trial shows that FCC can improve the amorphization kinetics of CAR. The faster amorphization kinetics can be attributed to FCC as a co-milling material, the accessibility of pores and surfaces of FCC to CAR molecules, including the formation of fresh surfaces from split FCC particles.

3.2. Solid state characterisation of CAR–FCC samples milled for 90 min

To characterise CAR–FCC samples, PM containing 10–80% CAR were milled for 90 min and DSC was used to measure the thermal response (Fig. 4). A $T_{g\alpha}$ signal was observed for all analysed samples. For CAR–FCC samples containing 10% CAR, a weak $T_{g\alpha}$ was observed at 49 °C. For CAR–FCC samples containing 20% CAR and above, a sigmoidal change in the heat flow was observed between 30 and 50 °C and an average $T_{g\alpha}$ value of 38 °C was found. This $T_{g\alpha}$ value is similar to that of neat CAR (37 °C [43]) and suggests deposition of CAR onto FCC as well as the presence of an amorphous CAR phase. Comparing the $T_{g\alpha}$ value of CAR–FCC samples containing 10% CAR to that of the other CAR–FCC samples, the 10% CAR sample has an approximately 11 °C higher $T_{g\alpha}$. This increased $T_{g\alpha}$ value can be attributed to restricted molecular mobility [27], since hindered molecular mobility has previously been found for drug molecules (amorphous CAR and ibuprofen) that are in close contact with their host particles (mesoporous silica) [34].

For CAR–FCC samples containing 40% CAR and above, an enthalpy recovery endotherm was seen superimposed on the $T_{g\alpha}$ signal, whereas for CAR–FCC samples containing 50–80% CAR, a recrystallization exotherm with an onset temperature of 86.3 ± 4.0 °C, was observed. For CAR–FCC samples containing 40% CAR and above, as the temperature was increased, a melting endotherm with an onset temperature at 106.3 ± 0.9 °C was observed. The melting endotherm corresponds to that of crystalline CAR with polymorphic form II [27]. The presence of a melting endotherm and enthalpy recovery for samples containing 40% CAR and above is an indication of the presence of pure amorphous CAR. This pure amorphous CAR phase is classified as excess CAR molecules [27,34]. These excess CAR molecules are mobile and can reorient themselves to recrystallize [27,34]. From the DSC analysis, it can be concluded that amorphous CAR can be obtained when CAR is milled with FCC, and ratios at and below 30% CAR can be stabilized with FCC, and thus the maximum drug load will be somewhere between 30 and 40% CAR.

3.3. Physical stability of CAR–FCC samples after different milling times

To determine the physical stability of CAR–FCC samples milled for 90 min, freshly prepared samples were stored at 100 °C for 2 h. The diffractograms of the various samples are shown in Fig. 5. Samples that contained 40% CAR and above showed diffraction peaks of crystalline CAR. This indicates the presence of excess CAR that is not deposited

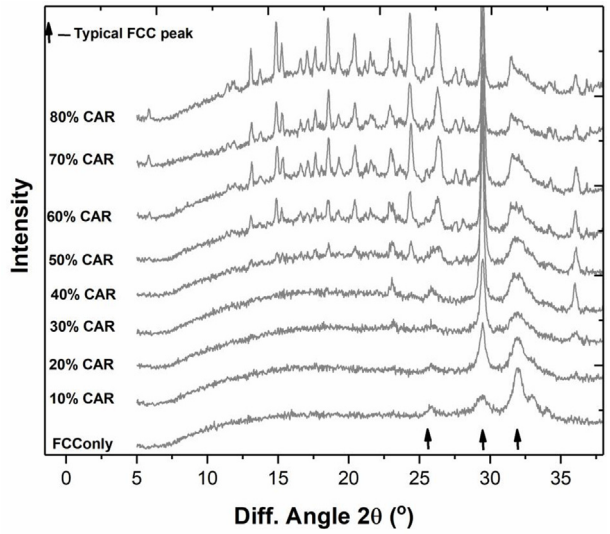

Fig. 5. Diffractograms of CAR–FCC samples containing 10–80% CAR and FCC milled for 90 min, after storage for 2 h at 100 °C. The diffractograms show absence of CAR peaks for samples with 10–30% CAR whilst they are present for samples with 40% CAR and above.

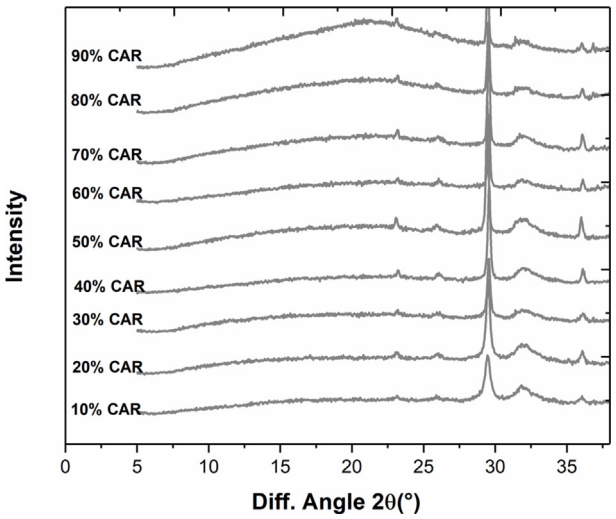

Fig. 6. Diffractograms of various CAR–FCC samples showing the disappearance of CAR peaks after milling for 30 min.

onto or interacting with the surface of FCC and hence recrystallizes [27,34]. Samples containing 30% CAR and below did not show diffraction peaks of CAR, however, typical FCC crystalline peaks are present in all the samples. This shows that the maximum ratio of CAR that can be adsorbed onto FCC is between 30 and 40% CAR and that the crystallinity of FCC does not have a negative effect on crystallization of CAR.

Since our initial trials showed that the CAR–FCC sample containing 50% CAR, became amorphous after only 10 min of milling, fresh CAR–FCC samples containing 10–90% CAR were milled for 30 min. The physical stability of the resulting samples at 25 °C under dry conditions were studied. The XRPD diffractograms (Fig. 6) show that at all drug to FCC ratios, CAR was amorphous.

The results of the physical stability study are shown in Fig. 7. Neat amorphous CAR and CAR–FCC samples containing 90–70% CAR were not stable and recrystallized in less than one week. CAR–FCC samples containing 60–50% drug were stable for one week (see Fig. S2 in supporting information). However, CAR–FCC samples containing 40% CAR were stable for 11 weeks and CAR–FCC samples containing 10–30% CAR were stable for the full tested time period of 19 weeks. This is in agreement with studies which found that CAR (up to 40% CAR), when

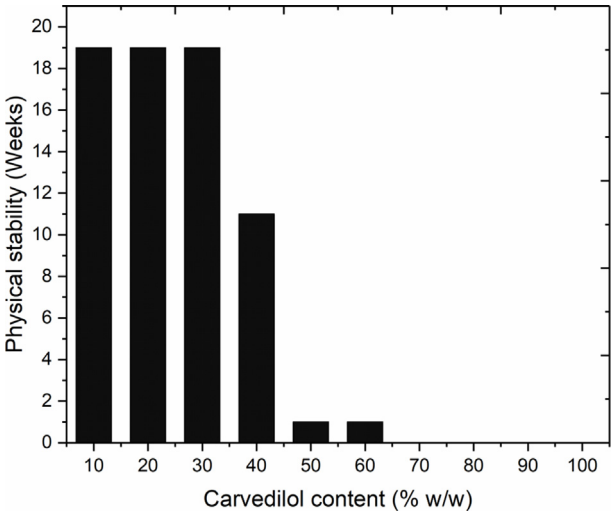

Fig. 7. Barchart showing the physical stability, measured in weeks, of CAR–FCC samples containing different CAR content milled for 30 min and stored under dry conditions at 25 °C.

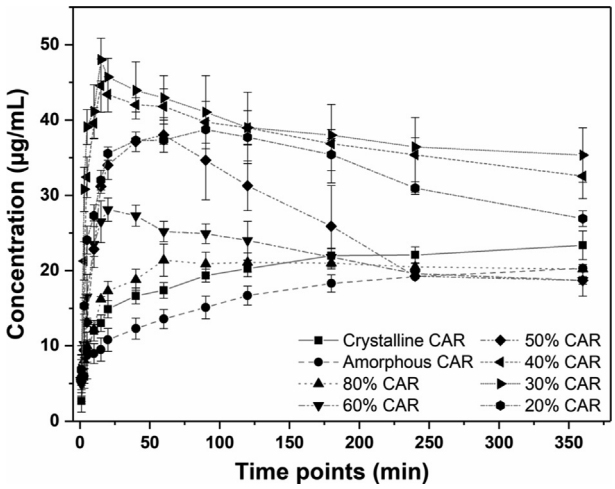

Fig. 8. Drug release profiles of crystalline CAR, amorphous CAR and various CAR–FCC samples.

melt loaded into mesoporous silica (6–35 nm pore sizes), remained physically stable [44]. The two stability tests revealed that CAR–FCC samples containing 10–30% CAR will be the most stable systems. The maximum drug load was determined from samples with the highest drug concentration that neither showed XRPD peaks of CAR after physical stability analysis, nor a DSC melting endotherm, and the sample with the lowest drug concentration that showed both, CAR XRPD peaks and a corresponding DSC melting endotherm. The maximum drug concentration for CAR–FCC samples is thus between 30 and 40% CAR.

3.4. Drug release of CAR–FCC samples milled for 30 min

In vitro drug release was investigated using powder dissolution of CAR–FCC samples containing different drug concentrations (milled for 30 min), pure crystalline and amorphous CAR powder samples. The results are shown in Fig. 8. Drug released for the first minute from neat amorphous CAR was over 2 fold higher than that of crystalline CAR, however thereafter, amorphous CAR failed to further improve the dissolution performance of the pure drug compared with crystalline CAR. This phenomenon is due to solid state conversion from the amorphous form of the drug to the crystalline form which happens within the first minutes upon contact with the dissolution media [45,46]. Poor drug release was also observed for CAR–FCC sample containing 80% CAR, and the release profile was comparable to that of crystalline CAR. CAR–FCC samples containing 60 and 50% CAR showed a comparatively higher drug release and supersaturation but after 360 min of dissolution, the released drug concentrations were similar to that of the amorphous CAR.

For CAR–FCC samples containing 40, 30 and 20% CAR, drug release increased gradually, reaching a maximum concentration after 20 min. The released drug concentration at this timepoint was 3 fold higher compared to crystalline CAR. These samples were able to maintain supersaturation for a long time and showed a higher released drug concentration within the 360 min of the dissolution experiment, compared with crystalline and amorphous CAR. The highest initial released drug concentration and the longest time of supersaturation were obtained for CAR–FCC samples containing 30 and 40% CAR. Whilst further studies are required to fully understand mechanisms involved in FCC water absorption, desorption of drug molecules and into the generation and maintaining of supersaturated drug systems, it can be stated that FCC improved the amorphous drug dissolution properties.

In summary, mechanochemical activation of CAR and FCC, produced amorphous CAR. Solid state analysis showed that CAR–FCC samples containing 30% CAR and below will be the most stable. Drug

release profile showed that a supersaturated system can be formed and maintained at these drug concentrations. This indicates a direct link between solid state properties of the samples and their release profiles in that, physically stable amorphous formulations can improve the solubility of poorly water soluble drugs. Therefore, the use of FCC as a co-former plays a significant role in improving drug amorphization kinetics, physical stability as well as improving the drug dissolution properties and supersaturation of CAR.

4. Conclusions

In this study, the amorphization of CAR was achieved by ball milling in the presence of FCC. The solid state of CAR–FCC samples was investigated by XRPD and DSC, and the physical stability and drug release from the CAR–FCC samples were assessed. It was found that for CAR–FCC samples containing 50% CAR, a milling time of 10 min was sufficient to convert CAR from the crystalline state into an amorphous form. Various CAR–FCC samples containing 20–80% CAR milled for 90 min had a similar $T_{g\alpha}$, which is an indication of deposition of amorphous drug on the surface of FCC particles. However, an increase in $T_{g\alpha}$ was observed for the sample with 10% CAR, suggesting impeded molecular mobility due to close proximity of CAR molecules to the FCC surface. Physical stability analysis, both under stress (100 °C) and non-stress storage conditions (25 °C at dry conditions), for CAR–FCC samples milled for either 30 or 90 min showed that, samples containing 30% CAR and below can be stabilized and maintained the longest time in an amorphous form compared to the samples with higher drug concentrations. Based on the absence or presence of CAR diffraction peaks after physical stability analysis and corresponding melting endotherms, the maximum drug load is between 30 and 40% drug ratio. *In vitro* drug release studies revealed that CAR–FCC samples containing 60% CAR and below can improve drug dissolution properties and produce supersaturated systems. However, for CAR–FCC samples containing 60 and 50% CAR, the drug recrystallizes or precipitates. In contrast, supersaturation is maintained for CAR–FCC samples that are physically stable. Mechanochemical activation using FCC is useful in improving amorphous drug stability and dissolution.

Declaration of Competing Interest

The authors declare no conflict of interest.

Acknowledgement

The authors acknowledge funding from NordForsk for the Nordic University Hub project #85352 (Nordic POP, Patient Oriented Products). Jingwen Liu acknowledges the China Scholarship Council (201806350247) for financial support. Daniel Markl is thanked for providing FCC (Omyapharm ® 500-OG).

Appendix A. Supplementary material

Supplementary data to this article can be found online at https://doi.org/10.1016/j.ejpb.2020.07.029.

References

[1] L. Di, E.H. Kerns, Chapter 8 - Permeability, in: L. Di, E.H. Kerns (Eds.), Drug-Like Properties, 2nd ed., Academic Press, Boston, 2016, pp. 95–111.
[2] L. Di, E.H. Kerns, Chapter 7 - Solubility, in: L. Di, E.H. Kerns (Eds.), Drug-Like Properties, 2nd ed., Academic Press, Boston, 2016, pp. 61–93.
[3] G.L. Amidon, H. Lennernas, V.P. Shah, J.R. Crison, A theoretical basis for a biopharmaceutic drug classification: the correlation of *in vitro* drug product dissolution and *in vivo* bioavailability, Pharm. Res. 12 (1995) 413–420, https://doi.org/10.1023/A:1016212804288.
[4] H.D. Williams, N.L. Trevaskis, S.A. Charman, R.M. Shanker, W.N. Charman, C.W. Pouton, C.J.H. Porter, Strategies to address low drug solubility in discovery and development, Pharmacol. Rev. 65 (2013) 315–499, https://doi.org/10.1124/pr.112.005660.
[5] J. Siepmann, F. Siepmann, Sink conditions do not guarantee the absence of saturation effects, Int. J. Pharm. 577 (2020) 119009, , https://doi.org/10.1016/j.ijpharm.2019.119009.
[6] G. Van den Mooter, The use of amorphous solid dispersions: A formulation strategy to overcome poor solubility and dissolution rate, Drug Discov. Today: Technol. 9 (2012) e79–e85, https://doi.org/10.1016/j.ddtec.2011.10.002.
[7] C. Leuner, J. Dressman, Improving drug solubility for oral delivery using solid dispersions, Eur. J. Pharm. Biopharm. 50 (2000) 47–60, https://doi.org/10.1016/S0939-6411(00)00076-X.
[8] Y. Perrie, T. Rades, FASTtrack Pharmaceutics: Drug Delivery and Targeting, Pharmaceutical press, London, UK, 2012.
[9] R.A. Bellantone, Fundamentals of Amorphous Systems: Thermodynamic Aspects, in: N. Shah, H. Sandhu, D.S. Choi, H. Chokshi, A.W. Malick (Eds.), Amorphous Solid Dispersions: Theory and Practice, Springer, New York, New York, 2014, pp. 3–34.
[10] T. Rades, K.C. Gordon, K. Graeser, A. Hassan, Molecular Structure, Properties, and States of Matter, in: L.A. Felton (Ed.), Remington: The Science and Practice of Pharmacy, Pharmaceutical Press, London, United Kingdom, 2013, pp. 117–206.
[11] E.O. Kissi, H. Grohganz, K. Löbmann, M.T. Ruggiero, J.A. Zeitler, T. Rades, Glass-transition temperature of the beta-relaxation as the major predictive parameter for recrystallization of neat amorphous drugs, J. Phys. Chem. B 122 (2018) 2803–2808, https://doi.org/10.1021/acs.jpcb.7b10105.
[12] M. Rams-Baron, R. Jachowicz, E. Boldyreva, D. Zhou, W. Jamroz, M. Paluch, Physical Instability: A Key Problem of Amorphous Drugs, in: M. Rams-Baron, R. Jachowicz, E. Boldyreva, D. Zhou, W. Jamroz, M. Paluch (Eds.), Amorphous Drugs: Benefits and Challenges, Springer International Publishing, Cham, 2018, pp. 107–157.
[13] R. Laitinen, P.A. Priemel, S. Surwase, K. Graeser, C.J. Strachan, H. Grohganz, T. Rades, Theoretical Considerations in Developing Amorphous Solid Dispersions, in: N. Shah, H. Sandhu, D.S. Choi, H. Chokshi, A.W. Malick (Eds.), Amorphous Solid Dispersions: Theory and Practice, Springer, New York, New York, 2014, pp. 35–90.
[14] S.R.K. Vaka, M.M. Bommana, D. Desai, J. Djordjevic, W. Phuapradit, N. Shah, Excipients for Amorphous Solid Dispersions, in: N. Shah, H. Sandhu, D.S. Choi, H. Chokshi, A.W. Malick (Eds.), Amorphous Solid Dispersions: Theory and Practice, Springer, New York, New York, 2014, pp. 123–161.
[15] S.J. Dengale, H. Grohganz, T. Rades, K. Löbmann, Recent advances in co-amorphous drug formulations, Adv. Drug Deliv. Rev. 100 (2016) 116–125, https://doi.org/10.1016/j.addr.2015.12.009.
[16] J. Siepmann, A. Faham, S.-D. Clas, B.J. Boyd, V. Jannin, A. Bernkop-Schnürch, H. Zhao, S. Lecommandoux, J.C. Evans, C. Allen, O.M. Merkel, G. Costabile, M.R. Alexander, R.D. Wildman, C.J. Roberts, J.-C. Leroux, Lipids and polymers in pharmaceutical technology: Lifelong companions, Int. J. Pharm. 558 (2019) 128–142, https://doi.org/10.1016/j.ijpharm.2018.12.080.
[17] S. Baghel, H. Cathcart, N.J. O'Reilly, Polymeric amorphous solid dispersions: A review of amorphization, crystallization, stabilization, solid-state characterization, and aqueous solubilization of biopharmaceutical classification system class II drugs, J. Pharm. Sci. 105 (2016) 2527–2544, https://doi.org/10.1016/j.xphs.2015.10.008.
[18] P.J. Marsac, S.L. Shamblin, L.S. Taylor, Theoretical and practical approaches for prediction of drug–polymer miscibility and solubility, Pharm. Res. 23 (2006) 2417–2426, https://doi.org/10.1007/s11095-006-9063-9.
[19] D. Medarević, J. Djuriš, P. Barmpalexis, K. Kachrimanis, S. Ibrić, Analytical and computational methods for the estimation of drug-polymer solubility and miscibility in solid dispersions development, Pharmaceutics 11 (2019) 372, https://doi.org/10.3390/pharmaceutics11080372.
[20] K. Löbmann, H. Grohganz, R. Laitinen, C. Strachan, T. Rades, Amino acids as co-amorphous stabilizers for poorly water soluble drugs – Part 1: Preparation, stability and dissolution enhancement, Eur. J. Pharm. Biopharm. 85 (2013) 873–881, https://doi.org/10.1016/j.ejpb.2013.03.014.
[21] W. Wu, H. Ueda, K. Löbmann, T. Rades, H. Grohganz, Organic acids as co-formers for co-amorphous systems – Influence of variation in molar ratio on the physicochemical properties of the co-amorphous systems, Eur. J. Pharm. Biopharm. 131 (2018) 25–32, https://doi.org/10.1016/j.ejpb.2018.07.016.
[22] W. Wu, K. Löbmann, J. Schnitzkewitz, A. Knuhtsen, D.S. Pedersen, T. Rades, H. Grohganz, Dipeptides as co-formers in co-amorphous systems, Eur. J. Pharm. Biopharm. 134 (2019) 68–76, https://doi.org/10.1016/j.ejpb.2018.11.016.
[23] R. Laitinen, K. Löbmann, C.J. Strachan, H. Grohganz, T. Rades, Emerging trends in the stabilization of amorphous drugs, Int. J. Pharm. 453 (2013) 65–79, https://doi.org/10.1016/j.ijpharm.2012.04.066.
[24] K. Löbmann, R. Laitinen, H. Grohganz, K.C. Gordon, C. Strachan, T. Rades, Coamorphous drug systems: enhanced physical stability and dissolution rate of indomethacin and naproxen, Mol. Pharmaceutics 8 (2011) 1919–1928, https://doi.org/10.1021/mp2002973.
[25] E.O. Kissi, K. Khorami, T. Rades, Determination of Stable Co-Amorphous Drug-Drug Ratios from the Eutectic Behavior of Crystalline Physical Mixtures, Pharmaceutics 11 (2019), https://doi.org/10.3390/pharmaceutics11120628.
[26] K. Löbmann, K.T. Jensen, R. Laitinen, T. Rades, C.J. Strachan, H. Grohganz, Stabilized Amorphous Solid Dispersions with Small Molecule Excipients, in: N. Shah, H. Sandhu, D.S. Choi, H. Chokshi, A.W. Malick (Eds.), Amorphous Solid Dispersions: Theory and Practice, Springer, New York, New York, 2014, pp. 613–636.
[27] E.O. Kissi, G. Kasten, K. Löbmann, T. Rades, H. Grohganz, The role of glass transition temperatures in coamorphous drug-amino acid formulations, Mol. Pharmaceutics 15 (2018) 4247–4256, https://doi.org/10.1021/acs.molpharmaceut.8b00650.
[28] W. Wu, K. Lobmann, T. Rades, H. Grohganz, On the role of salt formation and

structural similarity of co-formers in co-amorphous drug delivery systems, Int. J. Pharm. 535 (2018) 86–94, https://doi.org/10.1016/j.ijpharm.2017.10.057.
[29] M. Martínez-Carmona, Y.K. Gun'ko, M. Vallet-Regí, Mesoporous silica materials as drug delivery: "The nightmare" of bacterial infection, Pharmaceutics 10 (2018) 279, https://doi.org/10.3390/pharmaceutics10040279.
[30] K.K. Qian, R.H. Bogner, Application of mesoporous silicon dioxide and silicate in oral amorphous drug delivery systems, J. Pharm. Sci. 101 (2012) 444–463, https://doi.org/10.1002/jps.22779.
[31] A.D. Trofimov, A.A. Ivanova, M.V. Zyuzin, A.S. Timin, Porous inorganic carriers based on silica, calcium carbonate and calcium phosphate for controlled/modulated drug delivery: Fresh outlook and future perspectives, Pharmaceutics 10 (2018) 167, https://doi.org/10.3390/pharmaceutics10040167.
[32] M. Farzan, R. Roth, G. Québatte, J. Schoelkopf, J. Huwyler, M. Puchkov, Loading of porous functionalized calcium carbonate microparticles: Distribution analysis with focused ion beam electron microscopy and mercury porosimetry, Pharmaceutics 11 (2019) 32, https://doi.org/10.3390/pharmaceutics11010032.
[33] Y. Choudhari, H. Hoefer, C. Libanati, F. Monsuur, W. McCarthy, Mesoporous silica drug delivery systems, in: N. Shah, H. Sandhu, D.S. Choi, H. Chokshi, A.W. Malick (Eds.), Amorphous Solid Dispersions: Theory and Practice, Springer, New York, New York, 2014, pp. 665–693.
[34] E.O. Kissi, M.T. Ruggiero, N.-J. Hempel, Z. Song, H. Grohganz, T. Rades, K. Löbmann, Characterising glass transition temperatures and glass dynamics in mesoporous silica-based amorphous drugs, Phys. Chem. Chem. Phys. 21 (2019) 19686–19694, https://doi.org/10.1039/C9CP01764J.
[35] C.J. Ridgway, P.A.C. Gane, J. Schoelkopf, Modified calcium carbonate coatings with rapid absorption and extensive liquid uptake capacity, Colloids Suf. A Physicochem. Eng. Asp. 236 (2004) 91–102, https://doi.org/10.1016/j.colsurfa.2003.12.030.
[36] R. Roth, J. Schoelkopf, J. Huwyler, M. Puchkov, Functionalized calcium carbonate microparticles for the delivery of proteins, Eur. J. Pharm. Biopharm. 122 (2018) 96–103, https://doi.org/10.1016/j.ejpb.2017.10.012.
[37] T. Stirnimann, N. Di Maiuta, D.E. Gerard, R. Alles, J. Huwyler, M. Puchkov, Functionalized calcium carbonate as a novel pharmaceutical excipient for the preparation of orally dispersible tablets, Pharm. Res. 30 (2013) 1915–1925, https://doi.org/10.1007/s11095-013-1034-3.
[38] H. Sandhu, N. Shah, H. Chokshi, A.W. Malick, Overview of Amorphous Solid Dispersion Technologies, in: N. Shah, H. Sandhu, D.S. Choi, H. Chokshi, A.W. Malick (Eds.), Amorphous Solid Dispersions: Theory and Practice, Springer, New York, New York, 2014, pp. 91–122.
[39] K.K. Qian, R.H. Bogner, Spontaneous crystalline-to-amorphous phase transformation of organic or medicinal compounds in the presence of porous media, part 1: thermodynamics of spontaneous amorphization, J. Pharm. Sci. 100 (2011) 2801–2815, https://doi.org/10.1002/jps.22519.
[40] N. Chieng, J. Aaltonen, D. Saville, T. Rades, Physical characterization and stability of amorphous indomethacin and ranitidine hydrochloride binary systems prepared by mechanical activation, Eur. J. Pharm. Biopharm. 71 (2009) 47–54, https://doi.org/10.1016/j.ejpb.2008.06.022.
[41] S. Klein, V.P. Shah, A standardized mini paddle apparatus as an alternative to the standard paddle, AAPS Pharm. 9 (2008) 1179–1184, https://doi.org/10.1208/s12249-008-9161-6.
[42] G. Kasten, H. Grohganz, T. Rades, K. Löbmann, Development of a screening method for co-amorphous formulations of drugs and amino acids, Eur. J. Pharm. Sci. 95 (2016) 28–35, https://doi.org/10.1016/j.ejps.2016.08.022.
[43] L.I. Blaabjerg, E. Lindenberg, K. Löbmann, H. Grohganz, T. Rades, Glass forming ability of amorphous drugs investigated by continuous cooling and isothermal transformation, Mol. Pharmaceutics 13 (2016) 3318–3325, https://doi.org/10.1021/acs.molpharmaceut.6b00650.
[44] N.-J. Hempel, K. Brede, N.E. Olesen, N. Genina, M.M. Knopp, K. Löbmann, A fast and reliable DSC-based method to determine the monomolecular loading capacity of drugs with good glass-forming ability in mesoporous silica, Int. J. Pharm. 544 (2018) 153–157, https://doi.org/10.1016/j.ijpharm.2018.04.035.
[45] O. Planinšek, B. Kovačič, F. Vrečer, Carvedilol dissolution improvement by preparation of solid dispersions with porous silica, Int. J. Pharm. 406 (2011) 41–48, https://doi.org/10.1016/j.ijpharm.2010.12.035.
[46] V.B. Pokharkar, L.P. Mandpe, M.N. Padamwar, A.A. Ambike, K.R. Mahadik, A. Paradkar, Development, characterization and stabilization of amorphous form of a low T_g drug, Powder Technol. 167 (2006) 20–25, https://doi.org/10.1016/j.powtec.2006.05.012.